JCTC Journal of Chemical Theory and Computation

Evaluation of Salt Bridge Structure and Energetics in Peptides Using Explicit, Implicit, and Hybrid Solvation Models

Asim Okur,[†] Lauren Wickstrom,[#] and Carlos Simmerling*[,†,#]

Department of Chemistry and Graduate Program in Biochemistry and Structural Biology, Stony Brook University, Stony Brook, New York 11794

Received September 11, 2007

Abstract: Replica exchange or parallel tempering molecular dynamics (REMD) is widely used to enhance the exploration of free energy landscapes for complex molecular systems. However its application to large systems is hampered by the scaling of the number of required replicas with an increasing system size. We recently proposed an improved REMD method where the exchange probabilities were calculated using a hybrid explicit/implicit solvent model. We previously tested this hybrid solvent REMD approach on alanine polypeptides of 1, 3, and 10 residues and obtained very good agreement with fully solvated REMD simulations while significantly reducing the number of replicas required. In this study we continue evaluating the applicability of the hybrid solvent REMD method through comparing the free energy of formation of ion pairs using model peptides. In accord with other studies, pure GB simulations resulted in overstabilized salt bridges, whereas the hybrid models produced free energy profiles in close agreement with fully solvated simulations, including solvent separated minima. Furthermore, the structure of the salt bridge in explicit solvent is reproduced by the hybrid solvent REMD method, while the GB simulations favor a different geometry.

Introduction

Conformational sampling remains one of the biggest challenges in atomistic simulations for biological systems. Rugged and complex energy surfaces often result in simulations being trapped even when a sufficiently accurate Hamiltonian is used, prohibiting complete exploration of the conformational space. Significant effort has been put into developing efficient simulation methods to locate low-energy minima for these complex systems. The challenges in conformational sampling have been discussed in several reviews.[1,2]

One major problem for molecular simulations is quasi-ergodicity where simulations may appear converged when observing some simulation parameters, but in reality large energy barriers may prevent them from sampling important regions of the energy landscape. Another simulation initiated in a different conformation may look converged as well, but comparison may show that only partial equilibration was achieved (see ref 3 as an example for quasi-ergodicity).

One popular approach to overcoming quasi-ergodicity in biomolecular simulation is the replica exchange method.[4−6] In replica exchange molecular dynamics (REMD)[7] (also known as parallel tempering[4]), a series of molecular dynamics simulations (replicas) is performed for the system of interest. In the original form of REMD, each replica is an independent realization of the system, coupled to a thermostat at a different temperature. The temperatures of the replicas span a range from low values of interest (experimentally accessible temperatures such as 280 or 300 K) up to high values (such as 600 K) at which the system is expected to more rapidly overcome potential energy barriers that would otherwise impede conformational transitions on a computationally affordable time scale.

At intervals during the otherwise standard simulations, conformations of the system being sampled at different temperatures are exchanged based on a Metropolis-type

* Corresponding author e-mail: carlos.simmerling@stonybrook.edu.
[†] Department of Chemistry.
[#] Graduate Program in Biochemistry and Structural Biology.

10.1021/ct7002308 CCC: $40.75
Published on Web 02/21/2008

criterion[8] that considers the probability of sampling each conformation at the alternate temperature (further details are discussed in Methods). In this manner, REMD is hampered to a lesser degree by the local minima problem, since simulations at low temperatures can escape kinetic traps by "jumping" directly to alternate minima being sampled at higher temperatures. Moreover, the transition probability is constructed such that the canonical ensemble properties are maintained during each simulation, thus providing potentially useful information about conformational probabilities as a function of temperature. Due to these advantages, REMD has been widely applied to folding studies of peptides and small proteins.[4,7,9−20]

For large systems, REMD can become intractable since the number of replicas needed to span a given temperature range increases with the square root of the number of degrees of freedom in the system.[21−24] Since the number of accessible conformations also typically increases with system size, the current computational cost for REMD simulations of large systems limits the simulation lengths to tens of nanoseconds per replica, which limits the ability to obtain converged ensembles for large systems. Several promising techniques have been proposed[21,25−35] to deal with this apparent disadvantage of REMD.

Continuum solvent models like the semianalytical Generalized Born (GB) model[36] estimate the free energy of solvation of the solute based on coordinates of the solute atoms. The neglect of explicit solvent molecules can significantly reduce the computational cost of evaluating energies and forces for the system, but a larger effect with REMD can arise from the reduction in the number of replicas due to fewer degrees of freedom. However, these models can also have significant limitations. Since the atomic detail of the solvent is not considered, modeling specific effects of structured water molecules can be challenging. In the case of protein and peptide folding, it appears likely that the current generation of GB models do not have as good a balance between protein−protein and protein−solvent interactions as do the more widely tested explicit solvent models.[37,38] Previous studies on alanine based peptides show that the use of GB models can induce some bias in helical backbone conformations.[29,39] More particularly, it has been reported[14,38,40,41] that ion pairs were frequently too stable in the GB implicit water model, causing salt bridged conformations to be oversampled in MD simulations, thus altering the thermodynamics and kinetics of folding for small peptides. A clear illustration was given by Zhou and Berne[38] who sampled the C-terminal β-hairpin of protein G (GB1) with both a surface-GB (SGB)[42] continuum model and explicit solvent. The lowest free energy state with SGB was significantly different from the lowest free energy state in explicit solvent, with non-native salt bridges formed at the core of the peptide, in place of hydrophobic contacts. Zhou extended this study on GB1 by examining several force field-GB model combinations, with all GB models tested showing erroneous salt bridges.[41] The helical backbone bias and overstabilized salt bridges prevent the use of these GB models for conformational search for peptides and proteins.

Recognizing that a major obstacle in applying REMD with explicit solvent lies in the number of simulations (replicas) required, rather than just the complexity of each simulation, we introduced a new approach in which each replica is simulated in explicit solvent using standard methods such as periodic boundary conditions and inclusion of long-range electrostatic interactions.[28] However, the calculation of exchange probabilities (which determines the temperature spacing and thus the number of replicas) is handled differently. Only a subset of closest water molecules is retained, with the remainder temporarily replaced by a continuum representation. The energy is calculated using the hybrid model, and the exchange probability is determined. The original solvent coordinates are then restored, and the simulation proceeds as a continuous trajectory with fully explicit solvation. This way the perceived system size for evaluation of exchange probability is dramatically reduced and fewer replicas are needed.

Earlier tests of our hybrid solvent REMD method were performed on alanine polymers of 1, 3, and 10 residues, and the performance of hybrid approach was compared to fully solvated explicit solvent REMD simulations.[28] For Ala_{10}, a fivefold reduction in the number of replicas provided similar exchange probability, and good agreement was found for the populations of various minima corresponding to secondary structure types. The explicit inclusion of the first solvation shell eliminated the helical backbone bias introduced by GB and resulted in distributions in close agreement with fully solvated simulations.[28]

A similar approach was developed by Liu et al.[43] where they identified the solute as the central group and separated solute−solvent interaction energies and solvent−solvent energies and made solvent−solvent energies temperature dependent (Replica Exchange with Solute Tempering − REST). On average the temperature-dependent water−water interactions cancel over the replicas, bringing the potential energy distributions closer and providing better overlap with fewer replicas. The REST approach was tested on alanine dipeptide simulations, and significant reduction in the required number of replicas was observed.[43] When REST was applied to larger systems, however, the method was not as efficient.[44] To help overcome this issue they included a subset of water molecules to the central group and calculated their interactions explicitly with the solute, thereby using the increased energy fluctuations from the water interactions to provide the thermal basis for driving solute conformation exchanges. To obtain similar results with fully solvated REMD however a significant number of random central waters had to be added. Since the resulting central group was still smaller than the whole system, some reduction in the number of replicas required was observed.[44]

We previously chose to study polyalanines since the lack of complex side-chain interactions in these peptides enabled direct evaluation of the effect of solvent model on backbone conformation distributions. The results demonstrated that the GB models introduce significant secondary structure bias even in the absence of more complex side-chain functional groups.[39] While the hybrid solvent approach largely corrected these problems, application to more complex systems

requires validation with interactions between side chains, particularly charge−charge interactions such as salt bridges, for which GB models have been shown to perform poorly.[45]

In this report we describe further testing of the hybrid approach on peptides with the possibility of interactions between oppositely charged side chains. We calculate the Potential of Mean Force (PMF) of salt bridge formation between Arg and Glu side chains in a small model peptide where the charged residues are separated by 2 alanine residues. The hybrid solvent REMD results are compared to fully TIP3P solvated REMD simulations and GB-REMD simulations on the same system. As we observed with polyalanine peptides, GB models induced a bias resulting in overpopulation of helical backbone conformations. In order to separate the effects of solvent model on backbone conformation from those involving the side chains, we repeated our evaluation of ion pairing in REMD simulations with restrained backbone conformations. With a consistent set of backbone conformations, the GB REMD simulations showed salt bridges that are 2−3 kcal/mol stronger than corresponding TIP3P REMD simulations, and the salt bridge orientation and hydrogen-bonding pattern also differed. The use of hybrid solvent REMD reduced the number of replicas by a factor of 5 compared to fully explicit water REMD while providing the same preferred salt bridge geometry as explicit solvent and also greatly improved the free energy profile for ion pairing compared to pure GB REMD.

To further validate this approach, we applied the hybrid REMD method on a larger system, HP-1, corresponding to the isolated N-terminal helix of villin headpiece helical subdomain HP36. Previous work on HP-1 showed ∼1.5 kcal/mol overstabilization of the α-helix conformation and a stronger salt bridge interaction in GB simulations compared to explicit solvent.[46] Here, we compare melting curves and free energy of salt bridge formation between Lys and Asp residues obtained with the hybrid solvent REMD approach to our previous data obtained using standard REMD in explicit or implicit water. The hybrid solvent REMD simulations showed a significant improvement in the population of helical conformations across a wide range of temperatures. The salt bridge PMFs obtained from hybrid solvent REMD were also in better agreement with explicit solvent including the solvent separated minimum and correct location of the global free energy minimum. The results from both peptides provide further validation of the hybrid solvent REMD approach for application to more complex systems.

Methods

Arg-Ala-Ala-Glu Model Peptide. We simulated a 4 residue model peptide (Arg-Ala-Ala-Glu) with acetylated and amidated N- and C-termini, respectively. All simulations employed Amber ff99SB,[47] a modified version of ff94/ff99[48,49] with corrections to dihedral parameters to improve secondary structure preferences. Explicit solvent and hybrid solvent REMD simulations used the TIP3P water model.[50] The standard REMD simulations in explicit solvent and in pure GB were run using our REMD implementation as distributed in Amber (version 9).[51] The hybrid solvent REMD calculations were performed with a locally modified version of Amber 9. All bonds involving hydrogen were constrained in length using SHAKE.[52] The time step was 2 fs. Temperatures were maintained using weak coupling[53] to a bath with a time constant of 0.5 ps^{-1}.

Explicit Solvent REMD. The model peptide was solvated in a truncated octahedron box with 16 Å buffer using 2286 TIP3P water molecules for a total of 6926 atoms. Such a large solvent box was selected to ensure that the salt bridge distance between images is larger than the maximum distance available for the linear peptide to reduce possible artifacts caused by periodicity.[54] The system was equilibrated at 300 K for 50 ps with harmonic positional restraints on solute atoms, followed by minimizations with gradually reduced solute positional restraints and three 5 ps MD simulations with gradually reduced restraints at 300 K. Long-range electrostatic interactions were calculated using PME.[55] Simulations were run in the NVT ensemble.

Forty-six replicas all starting from a salt bridged conformation were used at temperatures ranging from 296 K to 584 K, which were optimized to give a uniform exchange acceptance ratio of ∼25%. Exchange between neighboring temperatures was attempted every 1 ps, and each REMD simulation was run for 30 000 exchange attempts (30 ns per replica). The first 5000 exchange attempts of the simulation were discarded to remove initial structure bias.

Implicit Solvent REMD. Solvent effects were calculated through the use of the Generalized Born[36] implicit solvent model with the GB^{OBC} [56] implementation in Amber. The intrinsic Born radii were adopted from Bondi[57] with modification of hydrogen.[58] The GB^{OBC} model was employed with mbondi2 radii. Scaling factors were taken from the TINKER modeling package.[59] No cutoff on nonbonded interactions was used. All other simulation parameters were the same as used in explicit solvent.

For the model peptide, the use of the continuum solvent model resulted in a system size of 68 atoms which permitted the use of 6 replicas to cover a temperature range of 300−636 K. Exchanges were attempted every 1 ps, and the REMD simulations were run 30 000 exchange attempts (30 ns). The first 5000 exchanges were again removed. All replicas were initiated with the same initial peptide conformation used for the explicit solvent REMD calculations.

Hybrid Solvent REMD. All simulation parameters in the hybrid solvent REMD simulations were the same as those employed for standard REMD in explicit solvent, with the exception of the number of replicas (8 replicas were used to cover the temperature range from 270 K to 570 K). The hybrid solvent exchange scheme is employed exactly as described in ref 28. At each exchange step during hybrid solvent REMD, the distance between the oxygen atom of each water molecule and all solute atoms was calculated. Water molecules were then sorted by their closest solute distance, and all water molecules except the 75 with the shortest solvent−solute distances were temporarily discarded. Seventy-five water molecules were sufficient to solvate the first shell of the peptide in extended conformation (Figure S.1. in the Supporting Information). The energy of this smaller system was then recalculated using only these close waters, and the remainders were replaced by the GB solvent

model. This hybrid solvent energy was used to calculate the exchange probability, and then all waters were restored to their original positions and the simulations were continued. In this manner the simulations using the hybrid solvent model produce continuous trajectories with fully explicit solvent, and the hybrid model was used only during calculation of exchange probabilities. The hybrid exchange scheme significantly reduced the number of replicas required as compared to explicitly including all solvent in the exchange calculation (46 vs 8 replicas) while maintaining a similar exchange success ratio of 20−30% (the observed exchange ratios can be found in Table S.1. in the Supporting Information). We only included the first solvation shell in the present simulations since our previous work[28] suggested that retaining a second shell provided little additional benefit and significantly increased the system size.

Analysis. Salt bridge PMFs were calculated using histogram analysis along a reaction coordinate defined using the distance between the Cζ of Arg1 and Cδ of Glu4 for the model peptide. Using Cζ resulted in a PMF that was less sensitive to the particular H-bond donor of the guanidino group which was analyzed separately. All distances were calculated using the ptraj module in Amber 8. Due to the computational cost of the REMD simulations, particularly standard REMD in explicit water, only a single run was performed for each solvent model, and uncertainties were calculated from the difference between free energy values obtained using the first half of the data set and those obtained only from the second half of the simulation. The convergence of our simulations was further checked by ensuring the salt bridge was formed and broken multiple times for each replica (see Figure S.2. in the Supporting Information for salt bridge distances for sample replicas).

To compare the backbone conformations, cluster analysis over the backbone atoms was performed for temperature trajectories at 300 K obtained from each REMD simulation. The 300 K trajectories were combined, and cluster analysis was performed with Moil-View[60] using backbone atoms as a similarity criterion with average linkage. Clusters were then formed with the bottom-up approach using a similarity cutoff of 1.0 Å. In this approach, each structure was initially assigned to a distinct cluster, average rmsd values between all cluster pairs were calculated, and the cluster pair with the smallest rmsd was merged. This procedure was repeated until the most similar cluster pair exceeded the similarity cutoff. The population of each cluster was then calculated separately for each simulation and plotted against each other for easy comparison. The same clustering scheme was used to investigate salt bridge orientations between different models where the atoms of Arg and Glu side chains were clustered again with a similarity cutoff of 1.0 Å.

Restrained REMD simulations used the same procedure for unrestrained simulations where the backbone conformation was restrained to the representative conformation obtained from the highest populated TIP3P cluster using weak (1.0 kcal/mol*Å) positional restraints. Restrained REMD simulations were run up to 40 000 exchange attempts for each solvation method, and the first 5000 exchange attempts were discarded as equilibration.

HP-1 Model Peptide. The HP-1 REMD simulations were run in a similar manner as the Arg-Ala-Ala-Glu peptide. The system was built from the sequence MLSDEDFKAVFGM which corresponds to the N-terminal helix of the villin headpiece helical subdomain HP36 (pdb code 1VII).[61] We have investigated the structural ensembles of this peptide in an earlier study through well-converged explicit solvent REMD simulations.[46]

Hybrid solvent REMD simulations were performed using 100 explicit water molecules in the exchange calculations. Eight replicas with a temperature range from 272 to 539 K were started from the native helical conformation, and the simulation was run up to 40 ns per replica, where the first 10 ns was discarded for data analysis. The GB^{OBC} REMD simulations were run using the same number of replicas and temperature distributions and were run up to 40 ns. For the GB^{OBC} REMD simulations the first 10 ns was again discarded before analysis.

Melting curves were constructed by calculating the average fraction helicity for each temperature. Helical residues were selected based on DSSP criterion.[62] Salt bridge PMFs were calculated using histogram analysis along a reaction coordinate using the distance between Nζ of Lys48 and Cγ of Asp44. To reduce the effects of different backbone conformations for different solvation schemes, the salt bridge PMF was calculated at 365 K where, based on the melting curve, simulations using each solvent model showed similar helical propensities. Error bars were calculated by comparing the first half and the second half of the data sets.

Results and Discussion

We previously tested hybrid solvent REMD with polyalanine peptides of varying lengths, obtaining good agreement with standard explicit solvent REMD simulations at reduced cost.[28] In simulations using only GB solvation, strong α-helical populations were observed for alanine peptides with 3 and 10 residues, in disagreement with explicit solvent simulations. In contrast, use of hybrid solvent REMD provided secondary structure propensities in near quantitative agreement with standard explicit solvent REMD simulations. Cluster analysis of backbone conformations were also in good agreement between TIP3P and hybrid solvent REMD simulations, but pure GB solvation showed large errors in conformational preferences. These results indicated that GB introduces significant bias in peptide backbone conformations, even in the absence of more complex side-chain interactions.[39] To further validate the use of hybrid solvent REMD on more complex biopolymers we studied the interaction of side-chain ion pairs in a small model peptide Ace-Arg-Ala-Ala-Glu-NH2, with Arg and Glu both modeled in the charged state. Salt bridge strength in the various solvent models was evaluated through calculation of the potential of mean force for the distance between Cζ of Arg and Cδ of Glu as sampled in the simulated ensembles.

The model peptide was simulated with standard REMD using either the GB^{OBC} implicit water model or the TIP3P explicit water model. Hybrid solvent REMD simulations used the same procedure as previously described[28] where the MD portions of the REMD were performed using the same

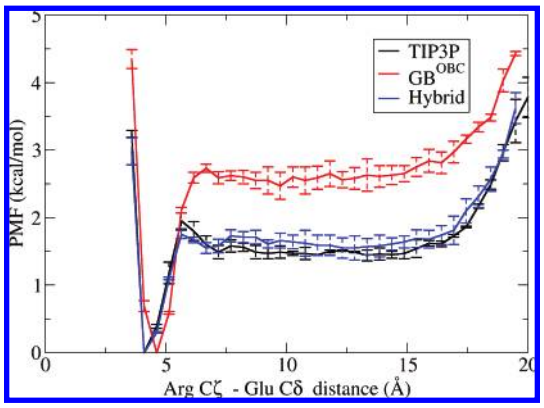

Figure 1. Potentials of mean force for the distance between Cζ of Arg and Cδ of Glu side chains to compare the free energy profiles for salt bridge formation for different methods. The GB^{OBC} method shows more stable salt bridges (~1.0 kcal/mol) compared to the TIP3P explicit solvent model. The hybrid solvent REMD method shows a profile similar to fully solvated TIP3P REMD.

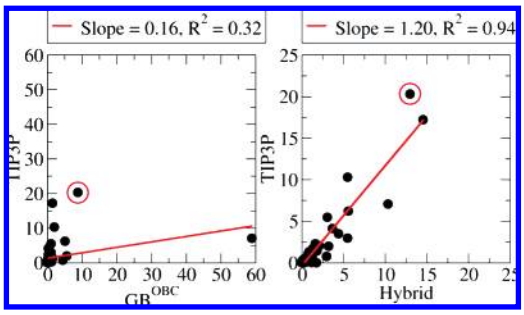

Figure 2. Comparison of backbone conformation populations for (left) standard REMD with GB^{OBC} and TIP3P (right) and standard REMD and hybrid solvent REMD simulations with TIP3P. Note that the scale differs for the right and left graphs, but the X and Y axes match in each graph. The slope and R^2 values for the best fit line are shown on top of each graph. Populations show poor correlation between TIP3P and GB^{OBC} ($R^2 = 0.32$) where the most populated conformation for GB^{OBC} has predominantly a helical conformation and is only weakly populated in TIP3P. In contrast, the populations of the conformational families show excellent correlation between the ensembles obtained through standard and hybrid solvent REMD ($R^2 = 0.94$). The most populated TIP3P REMD cluster is shown with red circles on each graph. (The populations for each cluster are provided in Table S.2. in the Supporting Information).

protocol and system as the standard REMD simulations in explicit water. The only difference was in the calculation of the exchange probability, during which all but the closest 75 water molecules were temporarily removed and replaced with the GB^{OBC} implicit model. All water molecules were restored to their original positions after the exchange calculation, thus the simulations provided continuous trajectories fully explicitly solvated during all MD steps. The use of the hybrid implicit/explicit solvent model during the exchange calculation dramatically reduced the number of replicas (from 46 to 8) required to obtain the desired exchange frequency.

The resulting salt bridge PMF curves for implicit, explicit, and hybrid solvent REMD are shown in Figure 1. The data demonstrate that the GB^{OBC} method produces modestly overstabilized salt bridges (about 1.0 kcal/mol) compared to explicit solvent, in accord with previous studies.[45] The GB^{OBC} profile also shows a free energy minimum at a slightly different value of distance than explicit solvent simulations, which suggests a different side-chain orientation or hydrogen bond pattern between solvent models. The PMF obtained from hybrid solvent REMD is very similar to the full TIP3P simulations, where both curves lie between their respective error bars, and also have their minimum at the same distance value. The curve follows the standard REMD TIP3P PMF closely over all distances sampled, including the prominent solvent separated minimum.

To investigate the differences in depth and location of the free energy minimum between the PMF profiles, we first compared the backbone conformations of the model peptide sampled with each solvation scheme. Knowing that this GB model introduces α-helical bias on the backbone of polyalanine peptides[28,39] we first looked at the backbone conformations from each solvation method to see if the helical bias in GB with polyalanine is also present with more complex side-chain functional groups. As described in the Methods section, we performed cluster analysis over the backbone atoms to identify multiple conformations sampled by each simulation. The temperature trajectories at 300 K from all 3 models were combined and clustered with a backbone rmsd cutoff of 1.0 Å, resulting in 63 clusters. The merging of the trajectory files for clustering allows direct comparison of populations between the different solvation approaches.[63] A comparison of the populations for each cluster in the different simulations is shown in Figure 2.

From Figure 2 we can readily observe that the GB and TIP3P solvent models sample very different backbone conformation ensembles. When the most populated conformations for each model are visually inspected, we observe that GB REMD predominantly samples a helical conformation (~60%) in accord with our previous simulations of alanine peptides.[39,63] Similar with the alanine peptides the extended conformation is the most populated backbone conformation for this model peptide.

Since the preferred backbone conformations are so different, it is difficult to identify the reason for different free energy profiles between GB^{OBC} and TIP3P. It is possible that the strong salt bridge and different orientation could be caused by the helical backbone conformation rather than the intrinsic energy profile of the ion pair. The improvements observed through the use of hybrid solvent REMD could also be because of better backbone sampling than with pure GB. To facilitate a more accurate comparison between the specific effects of solvation on the ion pair, we generated a new set of REMD simulations in which the backbone conformation was restrained to the representative conformation from the most populated TIP3P cluster (red circle in Figure 2). This comparison should eliminate any effects in the PMFs introduced by averaging over different backbone conformations and should give a more clear picture of salt bridge strength and orientation between TIP3P, GB^{OBC}, and hybrid solvent REMD.

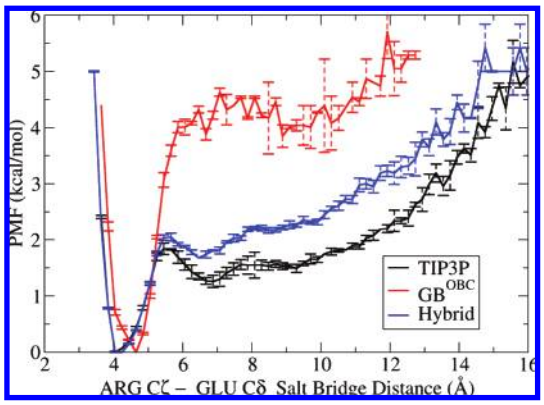

Figure 3. Potentials of mean force for salt bridge formation in the model peptide at 300 K for various solvation methods with restrained backbone conformation. Even with the backbone conformation restrained to that preferred in explicit solvent, GB^{OBC} still shows overstabilized salt bridges. The use of hybrid solvent REMD significantly improves the salt bridge free energy profile and identifies the minimum and solvent separated minimum correctly; however, the curve is shifted about 0.5 kcal/mol higher than with standard explicit solvent REMD.

The restrained REMD simulations were run for all three models for ~40 000 exchange attempts for each solvation scheme. The resulting PMF curves are shown in Figure 3. The hybrid solvent exchange criterion again provides data in good agreement with that from standard REMD in TIP3P; the hybrid solvent REMD profile is within 0.5−1 kcal/mol of the fully solvated TIP3P results over the entire range of distances. In contrast, the GB simulations show significant inaccuracies. Even after removal of possible bias from different backbone ensembles, the GB^{OBC} REMD data shows stronger salt bridge formation (2.5−3 kcal/mol) compared to the TIP3P standard REMD ensemble. It is interesting to note that this bias is even larger than the ~1 kcal/mol observed in Figure 1; the bias in backbone conformation with GB in the unrestrained ensemble appears to counteract the ion pair bias, indicating that unrestrained dynamics with GB has significant cancellation of error between inaccuracies in the secondary structure preferences and ion pair preferences that were not apparent without comparison of the backbone-restrained ensembles.

One of the common shortcomings of implicit solvation methods is the difficulty in modeling structured water molecules. In the case of ion pairs, solvent separated minima should be observed where the polar water molecule can hydrogen bond to and bridge the two ions. Such a minimum is clearly present at ~7 Å in the PMF curves obtained with standard REMD in explicit water (Figure 3; the minimum is not as apparent in Figure 1 due to averaging over profiles from many backbone conformations). The GB model used in the present study is a pairwise descreening model[64] and as such does not use a surface- or volume-based dielectric boundary. Therefore, no solvent separated minimum would be expected for this model, and none is observed in the PMF curves. Figure 3 shows that hybrid solvent REMD can identify the solvent separated minimum correctly, which is expected since the dynamics are carried out with full explicit

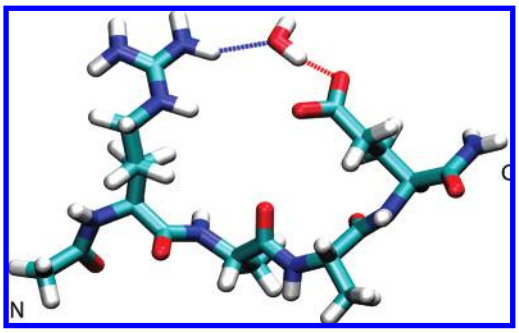

Figure 4. A sample structure snapshot from hybrid solvent REMD showing a water bridging the ion pair that results in a solvent separated minimum in the PMF curve in Figure 2. Other water molecules are present but not shown.

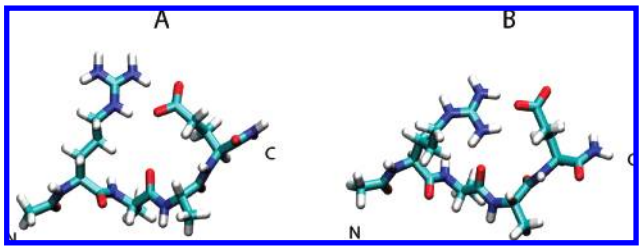

Figure 5. Representative structures of the most populated salt bridge geometries in standard REMD simulations using (A) TIP3P and (B) GB^{OBC}.

solvent and the first solvation shell is retained in the exchange probability calculation. Figure 4 shows a typical water bridged conformation obtained from the hybrid solvent REMD simulation. This is a key example showing that the inclusion of the first solvation shell can capture effects of water molecules close to protein surface explicitly without increasing the number of replicas required or the complexity of the GB calculation.

The free energy profiles for both restrained and unrestrained REMD simulations show about a 0.5 Å longer salt bridge distance in the GB ensemble as compared to that sampled in either standard or hybrid solvent REMD (Figures 2 and 3). The difference in both restrained and unrestrained backbone ensembles suggests that this shift to longer distances in GB REMD is a direct effect of GB and not a consequence of different salt bridge geometries with different backbone conformations. To investigate differences in geometry arising from GB, conformations with salt bridging present (salt bridge distance <5.5 Å) were subjected to cluster analysis for the heavy atoms participating in salt bridge formation in the backbone-restrained ensembles. Ten conformational clusters were obtained, two of which showed significant populations for all solvation schemes. The most populated cluster for the TIP3P and GB^{OBC} REMD simulations differed; the representative structure for these two clusters is shown in Figure 5.

Figure 5 shows the representative conformations for the most populated clusters. The first cluster (Figure 5A) is the most populated salt bridge conformation for the TIP3P simulations; about 65% of the structures that show a salt bridge adopt this conformation. The hybrid solvent REMD method is in excellent agreement with the standard TIP3P

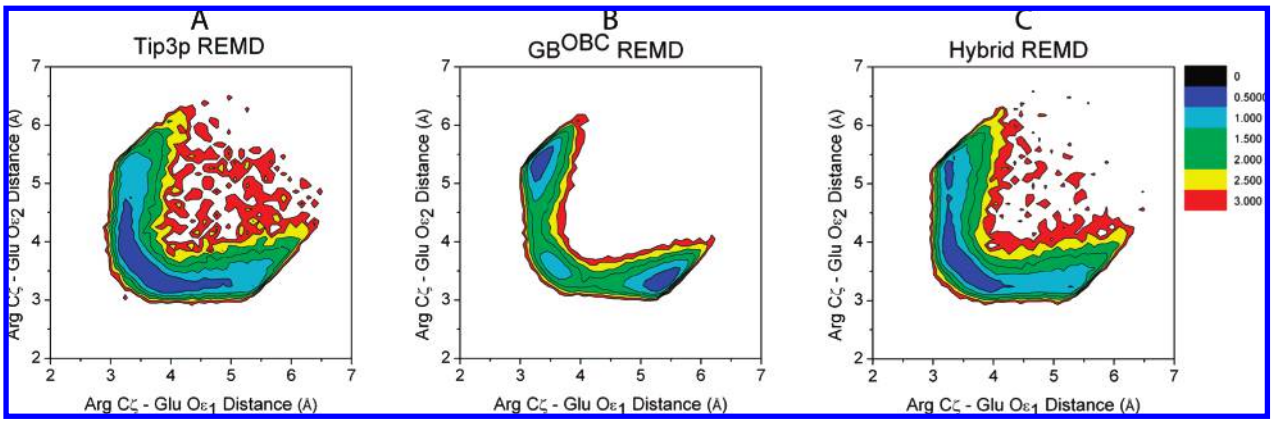

Figure 6. Free energy surfaces describing the geometry of salt bridge formation. The axes show the distance Arg Cζ and Glu $O\epsilon_1$ versus the distance Arg Cζ and Glu $O\epsilon_2$. Both standard (A) and hybrid solvent (C) REMD with TIP3P prefer that both oxygens simultaneously hydrogen bond with Arg, resulting in a single free energy minimum near the $x = y$-axis. In the GB simulations (B), there is a strong preference for a single oxygen to hydrogen bond to Arg, while the other remains solvent exposed, resulting a free energy minimum with one short and one long distance. Due to the symmetry of the carboxyl group, two such minima are present.

ensemble, with 52% of the salt bridging structures adopting this geometry. This preferred conformation is also the most populated cluster observed for Arg-Glu pairs in proteins, according to the Atlas of Protein Sidechain Interactions.[65]

In contrast, this geometry is only weakly sampled in the GB^{OBC} ensemble (8% of the salt bridging structures). Instead, the GB^{OBC} REMD simulations prefer the orientation shown in Figure 5B; over 70% of the structures adopt this alternate conformation in which the Arg side chain shows an 180° flip around the χ_4 dihedral angle as compared to the structure preferred in TIP3P. There is also a change in the Glu side chain, where one carboxyl oxygen faces out toward the (implicit) solvent and the other adopts a bifurcated hydrogen bond with Arg hydrogens. This GB-favored geometry between Arg and Glu side chains is not present among the top 6 orientations that are reported in the Atlas of Protein Sidechain Interactions. This conformation is only 23% populated in TIP3P simulations and about 40% in hybrid solvent REMD.

In order to further characterize the change in salt bridge geometry between simulations that do and do not include explicit water at the salt bridge interface, we investigated the hydrogen bond orientation between Arg and Glu side chains by calculating the 2-dimensional free energy profiles for the distances between Arg Cζ and the two Glu oxygens ($O\epsilon1$ $O\epsilon2$) for salt bridging conformations. In accord with cluster analysis results, the standard and hybrid solvent REMD simulations with TIP3P prefer that both Glu oxygens simultaneously have hydrogen bonds with the Arg. This is seen as one broad minimum in free energy where both oxygens adopt a comparable distance from the Arg Cζ (Figure 6A and C). However, GB^{OBC} prefers bifurcated hydrogen bonds between Arg and a single Glu oxygen, resulting in a preference for conformations with one of the Arg Cζ to Glu O distances longer than the other. Due to the symmetry of the Glu carboxyl group, this preference manifests as two free energy minima on the surface, as shown in Figure 6B. A small residual preference of less than 0.5 kcal/mol for the off-diagonal minimum remains with the hybrid solvent approach, although this is within the range of uncertainty in our data since only one of the two symmetric GB-like minima is comparable in free energy to the global free energy minimum. Overall, the hybrid solvent REMD surface is in much better agreement with that from TIP3P REMD than the GB surface. To further investigate this issue we compared the Arg χ_4 dihedral angle distributions between all solvent models. TIP3P and hybrid models show similar distributions in which multiple angles are nearly equally sampled. In contrast, the GB simulation shows a significantly greater preference for adopting a single rotamer (Figure S3).

The combined effect of different Arg−Glu geometries and hydrogen bond preference increases the salt bridge distance in GB ensembles by about 0.5 Å compared to those in standard or hybrid solvent REMD using TIP3P, which results in the difference in locations of free energy minima observed in the 1-dimensional PMF curves in Figures 1 and 3.

Further Testing Using the HP-1 Peptide. After successful tests with alanine peptides and the model peptide we performed a new set of simulations on a more complex peptide. The N-terminal helix of the villin headpiece helical subdomain HP36 (HP-1) is a 13 residue fragment with several charged residues that can form salt bridges. Previously we studied the structure of this fragment through converged explicit solvent REMD simulations which demonstrated that the fragment adopts a nativelike conformation in isolation.[46] In order to evaluate the general nature of observations for the short peptide described above, we performed pure GB^{OBC} and hybrid solvent REMD simulations for HP-1 and compared the results to our previous explicit solvent simulations. Figure 7 summarizes the comparison between each solvation scheme.

First we compared the differences in backbone conformations between the solvation schemes. We calculated the average helicity through DSSP analysis and compared the helical content of the fragment at each temperature (Figure 7A). Explicit solvent REMD shows a maximum ~27% helical content near 300 K. However the GB^{OBC} REMD

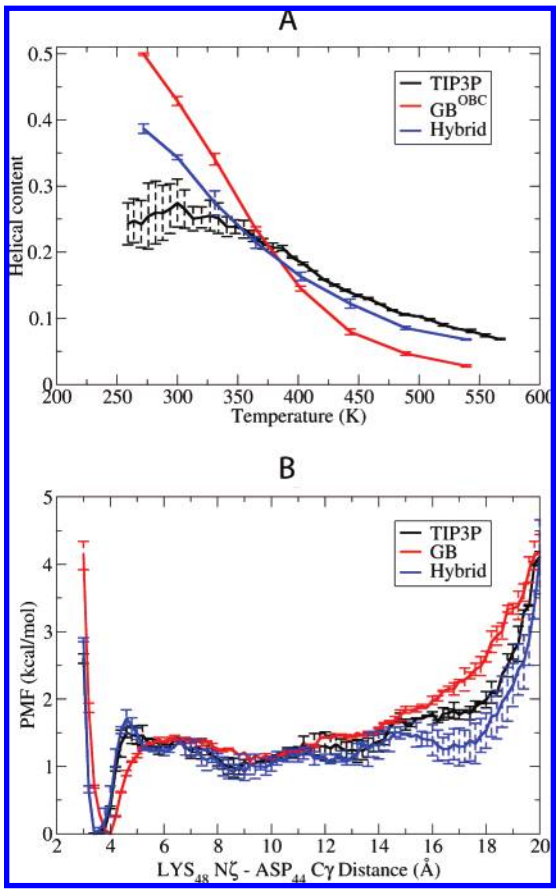

Figure 7. Melting profile (A) and salt bridge PMF (B) for the HP-1 fragment. The melting curve was calculated through average helicity determined through DSSP. At lower temperatures GB^{OBC} shows higher helical content than explicit solvent, while at higher temperatures GB^{OBC} underestimates the helical content. At higher temperatures hybrid solvent REMD is in excellent agreement with standard explicit solvent REMD; at lower temperatures the helical propensity tends to increase as is seen with GB^{OBC}, although the uncertainties in the explicit solvent data below 325 K make it difficult to evaluate this trend. The lower figure shows the PMF for salt bridge formation at 365 K. All solvent models show similar free energy profiles, but the hybrid solvent REMD data are in better agreement with the standard explicit solvent PMF, including the solvent separated minimum. GB^{OBC} also shows the same incorrect location of global minimum as was observed for the model peptide (Figures 1 and 3). This error is corrected in the hybrid model.

simulations show very high helical content at low temperatures (~45% at 300 K) as well as a significantly stronger temperature dependence of the helix population with more helix at low temperature and less helix at high temperature as compared to explicit solvent. Hybrid solvent REMD shows helical populations much closer to explicit solvent at lower temperatures, and the profile follows the explicit solvent profile very closely at higher temperatures. This shows that the hybrid REMD scheme is successful in reducing the backbone conformational bias of GB methods on more complicated sequences. The larger uncertainties in the standard REMD TIP3P data as compared to hybrid solvent REMD may arise from the use of more replicas in the standard REMD simulations and the longer time that it therefore requires for replicas to traverse the entire temperature range. However, even in the standard REMD simulations the largest uncertainties are only ±5%.

To reduce the effect of different backbone geometries we compared the PMFs for the salt bridge between Nζ of Lys48 and Cγ of Asp44 at 365 K (Figure 7B), since this temperature showed the closest agreement in helical content in the thermal profiles (Figure 7A). All solvent models show similar salt bridge free energy profile in terms of relative stability, but GB^{OBC} is again unable to reproduce the position of the global minimum and other details of the profile. The hybrid solvent REMD curve, however, is in very good agreement with standard explicit solvent REMD, successfully identifying the global minimum as well as the solvent separated minimum. Analysis of PMF curves at other temperatures shows similar trends (data not shown).

Conclusions

We studied the performance of the recently developed hybrid solvent REMD method on charged side chains, which have been shown to be problematic with GB implicit solvent models. We used a 4 residue peptide with charged Arg and Glu side chains separated by 2 Ala residues. Standard REMD simulations were performed with TIP3P explicit solvent and also with GB^{OBC} implicit solvent. Similar calculations were performed using hybrid solvent REMD using the same simulation system as the explicit water REMD, with the exception that REMD exchange probabilities were calculated using the 75 closest water molecules along with the GB^{OBC} model. The PMFs of salt bridge distances were calculated and compared for each approach. The GB^{OBC} model showed larger free energies of salt bridge formation compared to full explicit solvent REMD, indicating overstabilized salt bridges as previously observed. The GB simulations also show the same helical bias that we previously reported based on polyalanine simulations.[39,63] In addition to energetics, the GB simulations were unable to reproduce the correct salt bridge geometry; with ion pair and hydrogen bonding orientation is significantly different in GB-REMD simulations compared to TIP3P. Use of the hybrid solvation model in the exchange calculation significantly reduced the computational cost of REMD, while providing backbone conformational sampling, free energy profiles, and salt bridge geometries that were in excellent agreement with data from standard REMD in explicit solvent. Similar improvements in geometry and salt bridge PMFs were observed for the HP-1 model peptide.

As seen from salt bridge PMFs, the hybrid solvent REMD scheme performs very well with charged side chains. In both cases hybrid solvent REMD improves the PMFs with respect to TIP3P REMD simulations and nearly eliminates overstabilization introduced by GB models. However, a slight (0.5−1.0 kcal/mol) bias favoring salt bridge conformations remains in the hybrid model. Likewise, the 2-dimensional free energy surfaces describing salt bridge geometries also suggests a very small residual effect from the GB model, which was only used during the exchange calculation. Further studies will address whether even better agreement between standard explicit solvent and hybrid solvent REMD can be obtained

by improving the GB solvent model used in the hybrid approach or by replacing it with a more accurate method such as implicit solvent models based on the Poisson equation. Due to the infrequent need to calculate the hybrid solvent energy (every 500 MD steps in the present case), the additional computational overhead of more accurate implicit solvent models would be expected to have very little impact on the cost of the REMD simulation and still provide very significant savings as compared to standard REMD simulations in explicit solvent (a factor of 6 in the present case).

Acknowledgment. C.S. gratefully acknowledges financial support from the NIH (GM6167803) and supercomputer time at NCSA (NPACI MCA02N028).

Supporting Information Available: Temperature distributions and observed exchange ratios for all REMD simulations, table of populations and average errors shown in Figure 2, distributions of the number of water molecules within the first solvent shell at 300 K, distributions of the Arg Cζ−Glu Cδ salt bridge distance for 8 replicas for TIP3P REMD simulation, and distribution of Arg χ_4 dihedral angle for all solvent models. This material is available free of charge via the Internet at http://pubs.acs.org.

References

(1) Tai, K. Conformational sampling for the impatient. *Biophys. Chem.* **2004**, *107* (3), 213−220.

(2) Roitberg, A.; Simmerling, C. Special issue: Conformational sampling. *J. Mol. Graphics Modell.* **2004**, *22* (5), 317−317.

(3) Smith, L. J.; Daura, X.; van Gunsteren, W. F. Assessing equilibration and convergence in biomolecular simulations. *Proteins: Struct., Funct., Genet.* **2002**, *48* (3), 487−496.

(4) Hansmann, U. H. E. Parallel tempering algorithm for conformational studies of biological molecules. *Chem. Phys. Lett.* **1997**, *281* (1−3), 140−150.

(5) Swendsen, R. H.; Wang, J. S. Replica Monte-Carlo Simulation of Spin-Glasses. *Phys. Rev. Lett.* **1986**, *57* (21), 2607−2609.

(6) Tesi, M. C.; vanRensburg, E. J. J.; Orlandini, E.; Whittington, S. G. Monte Carlo study of the interacting self-avoiding walk model in three dimensions. *J. Stat. Phys.* **1996**, *82* (1−2), 155−181.

(7) Sugita, Y.; Okamoto, Y. Replica-exchange molecular dynamics method for protein folding. *Chem. Phys. Lett.* **1999**, *314* (1−2), 141−151.

(8) Metropolis, N.; Rosenbluth, A. W.; Rosenbluth, M. N.; Teller, A. H.; Teller, E. Equation of State Calculations by Fast Computing Machines. *J. Chem. Phys.* **1953**, *21* (6), 1087−1092.

(9) Feig, M.; Karanicolas, J.; Brooks, C. L. MMTSB Tool Set: enhanced sampling and multiscale modeling methods for applications in structural biology. *J. Mol. Graphics Modell.* **2004**, *22* (5), 377−395.

(10) Garcia, A. E.; Sanbonmatsu, K. Y. Exploring the energy landscape of a beta hairpin in explicit solvent. *Proteins: Struct., Funct., Genet.* **2001**, *42* (3), 345−354.

(11) Garcia, A. E.; Sanbonmatsu, K. Y. alpha-Helical stabilization by side chain shielding of backbone hydrogen bonds. *Proc. Natl. Acad. Sci. U.S.A.* **2002**, *99* (5), 2782−2787.

(12) Karanicolas, J.; Brooks, C. L. The structural basis for biphasic kinetics in the folding of the WW domain from a formin-binding protein: Lessons for protein design? *Proc. Natl. Acad. Sci. U.S.A.* **2003**, *100* (7), 3954−3959.

(13) Kinnear, B. S.; Jarrold, M. F.; Hansmann, U. H. E. All-atom generalized-ensemble simulations of small proteins. *J. Mol. Graphics Modell.* **2004**, *22* (5), 397−403.

(14) Pitera, J. W.; Swope, W. Understanding folding and design: Replica-exchange simulations of "Trp-cage" miniproteins. *Proc. Natl. Acad. Sci. U.S.A.* **2003**, *100* (13), 7587−7592.

(15) Roe, D. R.; Hornak, V.; Simmerling, C. Folding cooperativity in a three-stranded beta-sheet model. *J. Mol. Biol.* **2005**, *352* (2), 370−381.

(16) Sugita, Y.; Kitao, A.; Okamoto, Y. Multidimensional replica-exchange method for free-energy calculations. *J. Chem. Phys.* **2000**, *113* (15), 6042−6051.

(17) Zhou, R. H.; Berne, B. J.; Germain, R. The free energy landscape for beta hairpin folding in explicit water. *Proc. Natl. Acad. Sci. U.S.A.* **2001**, *98* (26), 14931−14936.

(18) Baumketner, A.; Shea, J. E. The structure of the Alzheimer amyloid beta 10−35 peptide probed through replica-exchange molecular dynamics simulations in explicit solvent. *J. Mol. Biol.* **2007**, *366* (1), 275−285.

(19) Paschek, D.; Nymeyer, H.; Garcia, A. E. Replica exchange simulation of reversible folding/unfolding of the Trp-cage miniprotein in explicit solvent: On the structure and possible role of internal water. *J. Struct. Biol.* **2007**, *157* (3), 524−533.

(20) Periole, X.; Mark, A. E. Convergence and sampling efficiency in replica exchange simulations of peptide folding in explicit solvent. *J. Chem. Phys.* **2007**, *126* (1).

(21) Cheng, X.; Cui, G.; Hornak, V.; Simmerling, C. Modified Replica Exchange Simulation Methods for Local Structure Refinement. *J. Phys. Chem. B* **2005**, *109* (16), 8220−8230.

(22) Fukunishi, H.; Watanabe, O.; Takada, S. On the Hamiltonian replica exchange method for efficient sampling of biomolecular systems: Application to protein structure prediction. *J. Chem. Phys.* **2002**, *116* (20), 9058−9067.

(23) Kofke, D. A. On the acceptance probability of replica-exchange Monte Carlo trials. *J. Chem. Phys.* **2002**, *117* (15), 6911−6914.

(24) Rathore, N.; Chopra, M.; de Pablo, J. J. Optimal allocation of replicas in parallel tempering simulations. *J. Chem. Phys.* **2005**, *122* (2), 024111.

(25) Jang, S. M.; Shin, S.; Pak, Y. Replica-exchange method using the generalized effective potential. *Phys. Rev. Lett.* **2003**, *91* (5), 058305.

(26) Mitsutake, A.; Sugita, Y.; Okamoto, Y. Replica-exchange multicanonical and multicanonical replica-exchange Monte Carlo simulations of peptides. I. Formulation and benchmark test. *J. Chem. Phys.* **2003**, *118* (14), 6664−6675.

(27) Sugita, Y.; Okamoto, Y. Replica-exchange multicanonical algorithm and multicanonical replica-exchange method for simulating systems with rough energy landscape. *Chem. Phys. Lett.* **2000**, *329* (3−4), 261−270.

(28) Okur, A.; Wickstrom, L.; Layten, M.; Geney, R.; Song, K.; Hornak, V.; Simmerling, C. Improved efficiency of replica exchange simulations through use of a hybrid explicit/implicit solvation model. *J. Chem. Theory Comput.* **2006**, *2* (2), 420−433.

(29) Okur, A.; Roe, D. R.; Cui, G. L.; Hornak, V.; Simmerling, C. Improving convergence of replica-exchange simulations through coupling to a high-temperature structure reservoir. *J. Chem. Theory Comput.* **2007**, *3* (2), 557−568.

(30) Roitberg, A. E.; Okur, A.; Simmerling, C. Coupling of replica exchange simulations to a non-Boltzmann structure reservoir. *J. Phys. Chem. B* **2007**, *111* (10), 2415−2418.

(31) Affentranger, R.; Tavernelli, I.; Di Iorio, E. E. A novel Hamiltonian replica exchange MD protocol to enhance protein conformational space sampling. *J. Chem. Theory Comput.* **2006**, *2* (2), 217−228.

(32) Lyman, E.; Zuckerman, D. M. Resolution exchange simulation with incremental coarsening. *J. Chem. Theory Comput.* **2006**, *2* (3), 656−666.

(33) Li, H.; Li, G.; Berg, B. A.; Yang, W. Finite reservoir replica exchange to enhance canonical sampling in rugged energy surfaces. *J. Chem. Phys.* **2006**, *125* (14), 144902.

(34) Li, H.; Yang, W. Sampling enhancement for the quantum mechanical potential based molecular dynamics simulations: a general algorithm and its extension for free energy calculation on rugged energy surface. *J. Chem. Phys.* **2007**, *126* (11), 114104.

(35) Min, D.; Li, H.; Li, G.; Bitetti-Putzer, R.; Yang, W. Synergistic approach to improve "alchemical" free energy calculation in rugged energy surface. *J. Chem. Phys.* **2007**, *126* (14), 144109.

(36) Still, W. C.; Tempczyk, A.; Hawley, R. C.; Hendrickson, T. Semianalytical Treatment of Solvation for Molecular Mechanics and Dynamics. *J. Am. Chem. Soc.* **1990**, *112* (16), 6127−6129.

(37) Nymeyer, H.; Garcia, A. E. Simulation of the folding equilibrium of alpha-helical peptides: A comparison of the generalized born approximation with explicit solvent. *Proc. Natl. Acad. Sci. U.S.A.* **2003**, *100* (24), 13934−13939.

(38) Zhou, R. H.; Berne, B. J. Can a continuum solvent model reproduce the free energy landscape of a beta-hairpin folding in water? *Proc. Natl. Acad. Sci. U.S.A.* **2002**, *99* (20), 12777−12782.

(39) Roe, D. R.; Okur, A.; Wickstrom, L.; Hornak, V.; Simmerling, C. Secondary structure bias in generalized born solvent models: Comparison of conformational ensembles and free energy of solvent polarization from explicit and implicit solvation. *J. Phys. Chem. B* **2007**, *111* (7), 1846−1857.

(40) Simmerling, C.; Strockbine, B.; Roitberg, A. E. All-atom structure prediction and folding simulations of a stable protein. *J. Am. Chem. Soc.* **2002**, *124* (38), 11258−11259.

(41) Zhou, R. H. Free energy landscape of protein folding in water: Explicit vs. implicit solvent. *Proteins: Struct., Funct., Genet.* **2003**, *53* (2), 148−161.

(42) Ghosh, A.; Rapp, C. S.; Friesner, R. A. Generalized born model based on a surface integral formulation. *J. Phys. Chem. B* **1998**, *102* (52), 10983−10990.

(43) Liu, P.; Kim, B.; Friesner, R. A.; Berne, B. J. Replica exchange with solute tempering: A method for sampling biological systems in explicit water. *Proc. Natl. Acad. Sci. U.S.A.* **2005**, *102* (39), 13749−13754.

(44) Huang, X.; Hagen, M.; Kim, B.; Friesner, R. A.; Zhou, R.; Berne, B. J. Replica Exchange with Solute Tempering: Efficiency in Large Scale Systems. *J. Phys. Chem. B* **2007**, *111* (19), 5405−5410.

(45) Geney, R.; Layten, M.; Gomperts, R.; Hornak, V.; Simmerling, C. Investigation of Salt Bridge Stability in a Generalized Born Solvent Model. *J. Chem. Theory Comput.* **2006**, *2* (1), 115−127.

(46) Wickstrom, L.; Okur, A.; Song, K.; Hornak, V.; Raleigh, D. P.; Simmerling, C. L. The Unfolded State of the Villin Headpiece Helical Subdomain: Computational Studies of the Role of Locally Stabilized Structure. *J. Mol. Biol.* **2006**, *360* (5), 1094−1107.

(47) Hornak, V.; Abel, R.; Okur, A.; Strockbine, B.; Roitberg, A.; Simmerling, C. Comparison of multiple Amber force fields and development of improved protein backbone parameters. *Proteins: Struct., Funct., Bioinformatics* **2006**, *65* (3), 712−725.

(48) Cornell, W. D.; Cieplak, P.; Bayly, C. I.; Gould, I. R.; Merz, K. M.; Ferguson, D. M.; Spellmeyer, D. C.; Fox, T.; Caldwell, J. W.; Kollman, P. A. A 2Nd Generation Force-Field for the Simulation of Proteins, Nucleic-Acids, and Organic-Molecules. *J. Am. Chem. Soc.* **1995**, *117* (19), 5179−5197.

(49) Wang, J. M.; Cieplak, P.; Kollman, P. A. How well does a restrained electrostatic potential (RESP) model perform in calculating conformational energies of organic and biological molecules? *J. Comput. Chem.* **2000**, *21* (12), 1049−1074.

(50) Jorgensen, W. L.; Chandrasekhar, J.; Madura, J. D.; Impey, R. W.; Klein, M. L. Comparison of Simple Potential Functions for Simulating Liquid Water. *J. Chem. Phys.* **1983**, *79* (2), 926−935.

(51) Case, D. A.; Cheatham, T. E.; Darden, T.; Gohlke, H.; Luo, R.; Merz, K. M.; Onufriev, A.; Simmerling, C.; Wang, B.; Woods, R. J. The Amber biomolecular simulation programs. *J. Comput. Chem.* **2005**, *26* (16), 1668−1688.

(52) Ryckaert, J. P.; Ciccotti, G.; Berendsen, H. J. C. Numerical-Integration of Cartesian Equations of Motion of a System with Constraints - Molecular-Dynamics of N-Alkanes. *J. Comput. Phys.* **1977**, *23* (3), 327−341.

(53) Berendsen, H. J. C.; Postma, J. P. M.; Vangunsteren, W. F.; Dinola, A.; Haak, J. R. Molecular-Dynamics with Coupling to an External Bath. *J. Chem. Phys.* **1984**, *81* (8), 3684−3690.

(54) Weber, W.; Hunenberger, P. H.; McCammon, J. A. Molecular dynamics simulations of a polyalanine octapeptide under Ewald boundary conditions: Influence of artificial periodicity on peptide conformation. *J. Phys. Chem. B* **2000**, *104* (15), 3668−3675.

(55) Darden, T.; York, D.; Pedersen, L. Particle Mesh Ewald - an N.Log(N) Method for Ewald Sums in Large Systems. *J. Chem. Phys.* **1993**, *98* (12), 10089−10092.

(56) Onufriev, A.; Bashford, D.; Case, D. A. Exploring protein native states and large-scale conformational changes with a modified generalized born model. *Proteins: Struct., Funct., Bioinformatics* **2004**, *55* (2), 383−394.

(57) Bondi, A. Van Der Waals Volumes + Radii. *J. Phys. Chem.* **1964**, *68* (3), 441−&.

(58) Tsui, V.; Case, D. A. Molecular dynamics simulations of nucleic acids with a generalized born solvation model. *J. Am. Chem. Soc.* **2000**, *122* (11), 2489−2498.

(59) Ponder, J. W.; Richards, F. M. An Efficient Newton-Like Method for Molecular Mechanics Energy Minimization of Large Molecules. *J. Comput. Chem.* **1987**, *8* (7), 1016−1024.

(60) Simmerling, C.; Elber, R.; Zhang, J. MOIL-View - A Program for Visualization of Structure and Dynamics of Biomolecules and STO - A Program for Computing Stochastic Paths. In *Modelling of Biomolecular Structures and Mechanisms*; Pullman et al., A., Ed.; Kluwer Academic Publishers: The Netherlands, 1995; pp 241−265.

(61) McKnight, C. J.; Matsudaira, P. T.; Kim, P. S. NMR structure of the 35-residue villin headpiece subdomain. *Nat. Struct. Biol.* **1997**, *4* (3), 180−4.

(62) Kabsch, W.; Sander, C. Dictionary of protein secondary structure: Pattern recognition of hydrogen-bonded and geometrical features. *Biopolymers* **1983**, *22* (12), 2577−2637.

(63) Okur, A.; Simmerling, C. Hybrid Implicit/Explicit Solvation Methods. In *Annual Reports in Computational Chemistry*; Elsevier: 2006; Vol. 2, pp 97−109.

(64) Hawkins, G. D.; Cramer, C. J.; Truhlar, D. G. Pairwise Solute Descreening of Solute Charges from a Dielectric Medium. *Chem. Phys. Lett.* **1995**, *246* (1−2), 122−129.

(65) Singh, J.; Thornton, J. M. In *Atlas of Protein Side-Chain Interactions*; IRL Press: Oxford, 1992; Vol. I & II.

CT7002308